Kim *et al. Applied Biological Chemistry* (2022) 65:80
https://doi.org/10.1186/s13765-022-00748-0

KSABC
The Korean Society for Applied Biological Chemistry

ARTICLE Open Access

Escherichia coli methionine-tRNAi/methionyl tRNA synthetase pairs induced protein initiation of interest (PII) expression

Jung Min Kim[1*†], Han Yong Lee[2†] and Jinho Jung[3]

Abstract

The precise regulatory role in protein synthesis by facilitating interactions with mRNA codons for various tRNA modifications is unclear. We previously reported that enhanced green fluorescent protein (GFP) reduced enhanced GFP mRNA expression in human methionine-conjugated initiator tRNA (tRNAi)/tRNA synthetase pairs under methionine-deficient conditions. Here, we investigated the effect of non-formylated methionine-conjugated *Escherichia coli* tRNAi on the synthesis of the protein initiation of interest (PII) in HeLa cells under intracellular L-methionine levels. We found that *E. coli* methionine-tRNAi counteracts human methionine-tRNAi, indicating that *E. coli* methionyl tRNA synthetase can induce enhanced GFP expression due to increased stability of enhanced GFP mRNA. Both complexes could support translation initiation without being employed to introduce methionine residues in the subsequent elongation steps. The results indicated that *E. coli* methionine-tRNAi could offset human methionine-tRNAi, and *E. coli* methionine-tRNAi/methionyl tRNA synthetase pairs can drive enhanced GFP mRNA expression. Unlike the human methionine-tRNAi/methionyl tRNA synthetase pairs that were used as a positive control, the non-formylated *E. coli* methionine-tRNAi/methionyl tRNA synthetase pairs reduced the expression of enhanced GFP mRNA, resulting in reduced HeLa cell survival. Using tRNAs functions causes of heterologous origin, such as from prokaryotes, and modified, to enhance or suppress the synthesis of specific proteins in eukaryotic organisms into the potential may possess a more prominent advantage of *E. coli* methionine-tRNAi as approaches that can control PII. This study provides new insights on the *E. coli* methionine- tRNAi/methionyl tRNA synthetase pair induced PII synthesis and the relative viability of cells could pave the way to regulate ecological/biological systems.

Keywords: Transfer RNA, *E. coli* initiator tRNA, Translation initiation, Non-formylated methionine, Formylated methionine, *E. coli* methionyl tRNA synthetase

Introduction

Protein engineering technologies based on cellular systems (e.g., mammalian, microbial [bacteria and yeast], insects, plants, and transgenic animals) have been developed on an industrial scale [1]. Protein intiation of interest (PII) expression is introduced into protein folding, post-translational modification, and product assembly, which are important biological activities in mammalian cells [2–5]. The introduction of PIIs based on large-scale recombinant protein production using gene or promoter transcriptional tools/resources and human codons has been expanded for high-efficiency protein expression [6–9].

To introduce PII expression in the cellular environment, amino acids containing methionine were integrated intracellular to obtain selective cellular metabolic labeling. The PII expression is an important component

†Jung Min Kim and Han Yong Lee contributed equally to this work

*Correspondence: jm77kim@korea.ac.kr; erine7.kim@gmail.com

[1] BK21 FOUR R&E Center for Environmental Science and Ecological Engineering, Korea University, Anam-ro145, Seongbuk-Gu, Seoul 02842, Republic of Korea
Full list of author information is available at the end of the article

of protein synthesis, post-translational modification, and product assembly, which are essential biological activities in mammalian cells [2–5]. Newly synthesized PII can occur through changes in both the structure and sequencing of tRNAi using an optimistic translation apparatus.

As one of the most complex biological processes involving cofactors and enzymes in cells, the initiation of protein synthesis can result in the production of various tRNAi motifs [10, 11]. tRNAi is typically used for the initiation of protein synthesis [12–14]. tRNAi carries essential structural elements, including anticodon loops, variable loops, acceptor stems, dihydrouridine loops, and T ψ (psi) C loops, through which they can target the ribosomal P sites of newly synthesized proteins [12, 13].

According to previous studies [15, 16], tRNAi imparts a unique structural conformation on the anticodon loop, which may be important for centering the tRNAi on the ribosomal P-site during the initiation of protein translation [12].

In *E. coli*, protein synthesis is generally initiated using fMet-tRNAi. In contrast, in eukaryotic organelles, such as mitochondria and chloroplasts, protein synthesis is initiated by Met-tRNAi. tRNAi is used solely to initiate protein translation, whereas elongator tRNA is used for inserting methionine during protein translation [12, 14]. tRNAi does not bind to elongation factors in the ribosomal A-site. Studies of the *E. coli* system revealed that fMet-tRNAis are charged by *E. coli* methionyl tRNA synthetase (EcMRS) [17, 18]. A strategy for cell-selective metabolic labeling of proteins in complex cellular mixtures using EcMRS (referred to as NLL-*Ec*MetRS) was reported in 2009 [18, 19]. The heterologous expression of human tRNAi using mutant EcMRS incorporates azidonorleucine (Anl) into proteins produced in HEK293 cells [17, 20]. This system can be used to engineer modified proteins for therapeutic and other applications, demonstrating the use of enrichment and visualization of proteins made at various stages of the cell cycle [17, 19].

Furthermore, tRNA modification promotes efficient and accurate translation, which influences the fidelity of protein synthesis, recognition by elongation aminoacyl tRNA synthetases (aaRS), and the efficiency of translation reading frames [21, 22].

Previous studies have revealed that fMet-tRNAi-dependent mistranslation could lead to protein degradation, an essential function in cellular homeostasis, and the destruction of anomalous proteins [23–25]. Aminoacyl tRNA has a high level of substrate selectivity and undergoes reliable synthesis by editing non-cognate products via selective aaRS activity [26]. Therefore, the pairing of cognate tRNAs in aaRS can be used to determine the fidelity of protein translation. The acceptor end of the tRNA molecule involved in the formation of the tRNAi/aaRS pair complex remains controversial [27, 28].

In addition, aaRS determines the genetic code of the amino acid pair by catalyzing the correct aminoacyl ester-linked tRNA process through a two-step reaction.

Therefore, the tRNA sequence motif in MRS has a high degree of specificity for methionine and can distinguish tRNAi molecules with similar structures [28–30]. Expansion of the tRNA species facilitates correct or mistranslation of the reading frame, selective genetic code, encoding translation, and engineered *E. coli* Met-tRNAi greatly improves our understanding of *E. coli* tRNAs.

Our study investigated protein synthesis by initiating the translational reading frames of *E. coli* tRNAi/aaRS pairs. A major function of methionine-containing amino acids is their action as substrates for the initiation of protein synthesis in mammalian cells [12, 31], where they play important roles in the regulation of cellular metabolism and proliferation rate; processes that are much more complex than protein synthesis. Similar to our fluorescent *E. coli* Met-tRNAi strategy, a green protocol and bactericidal biomaterial have recently been reported [32–34].

In this study, we investigated whether *E. coli* Met-tRNAi can initiate PII synthesis in HeLa cells. We hypothesized that protein synthesis initiation in eukaryotic cells is promoted via translation events involving *E. coli* Met-tRNAi/EcMRS pairs [35]. Here, we find and further support for the hypothesis that the association between protein synthesis initiation and a variety of initial-stage cell proliferation.

Materials and methods

Materials

Aminoacyl-tRNA synthetase from *Escherichia coli* (cat. no. 3646-10KU) and L-methionine (Met) (cat. no. M9625) were purchased from Sigma-Aldrich (St. Louis, MO, USA). In addition, 5-carboxyfluorescein (5-FAM), succinimidyl ester dye was purchased from Anaspec (San Jose, CA, USA) and used to fluorescently label the *E. coli* initiator methionine tRNA (*E. coli* tRNAi). tRNA was prepared using RNeasy Mini Kits (Qiagen, Hilden, Germany) and amplified by qRT-PCR. HeLa cells, obtained from American Tissue Type Collection (Manassas, VA, USA), were cultured in MEM (without phenol red) purchased from Welgene Inc. (Daegu, Republic of Korea). Lipofectamine 2000 was purchased from Invitrogen (Carlsbad, CA, USA).

In vitro human initiator tRNA and *E. coli* initiator tRNAs synthesis

The PCR product described above was used as a template for in vitro transcription [36] by T7 RNA polymerase

(Promega, Madison, WI, USA) to synthesize the *E. coli* initiator tRNA (tRNAi) sequences [16, 37] (Fig. 1). The conservation of the AUCG sequence among eukaryotic initiator tRNAs suggests that this sequence plays an essential role in the properties of initiator tRNAs (Additional file 1: Fig. S1A). The Watson–Crick base pair indicates unique characteristics at the end of the acceptor stem and the presence of a purine acceptor stem of *E. coli* initiator tRNAs (Additional file 1: Fig. S1B). Prokaryotic and eukaryotic initiator tRNAs include three guanines and three cysteines within the amino acid-anticodon stem, which form three GC pair repertories.

Modified initiator tRNA methionylation

To prepare human fluorophore-conjugated methionyl initiator tRNA (fluorescent Met-tRNAi) and *E. coli* fluorescent Met-tRNAi, the in vitro transcribed human initiator tRNAs were aminoacylated with purified fluorophore-conjugated methionine using refined human MRS [38] in the reaction buffer. The fluorophore 5-FAM added to the Met-tRNA(Met) after aminoacylation. The methionylation process was conducted in a reaction mixture containing 30 mM HEPES (pH 7.4), 100 mM potassium acetate, 10 mM magnesium acetate, and 100 mM ATP to produce the methionine-charged initiator tRNA. The *E. coli* initiator tRNAs were aminoacylated with purified fluorescent-labeled methionine, using purified preparations of *E. coli* methionyl-tRNA synthetase (MRS) and human MRS. After incubation at 37 °C for 10 min, 0.1 volume of 2.5 M NaOAc (pH 4.5) was added to the reaction mixture. *E. coli* tRNA was then extracted with 10 mM phenol-saturated NaOAc (pH 4.5), ethanol-precipitated, and centrifuged. The fluorescent-labeled methionine *E. coli* tRNAi in the pellet was dissolved in RNase-free water for subsequent methionylation of the human initiator tRNA.

Isolation of fluorescent-labeled methionine-charged initiator tRNA

The amine reactive group of the N-terminal methionine was conjugated with the fluorophore Cy5 (GE Healthcare, Piscataway, NJ) and 5-FAM dye (Sigma-Aldrich, St Louis, MO, USA). Fluorophore-conjugated methionine was prepared by conjugating the α-amino group of L-methionine with 5-FAM dye. Briefly, 0.1 mg of 5-FAM NHS ester dye was dissolved in 0.1 ml of 62.5 mM sodium tetraborate buffer (pH 8.5). After adding about 1 mg of L-methionine in 62.5 mM sodium tetraborate buffer (pH 8.5, 1.0 mL) at room temperature, the mixture was incubated overnight.

Analysis of L-methionine (L-Met) and fluorophore-conjugated methionine with high-performance liquid chromatography

The in vitro transcription of human tRNAi (73 base pairs) and charged methionine *E. coli* tRNAi, using T7 RNA polymerase (Promega, Madison, WI, USA), was detected by agarose gel separation and

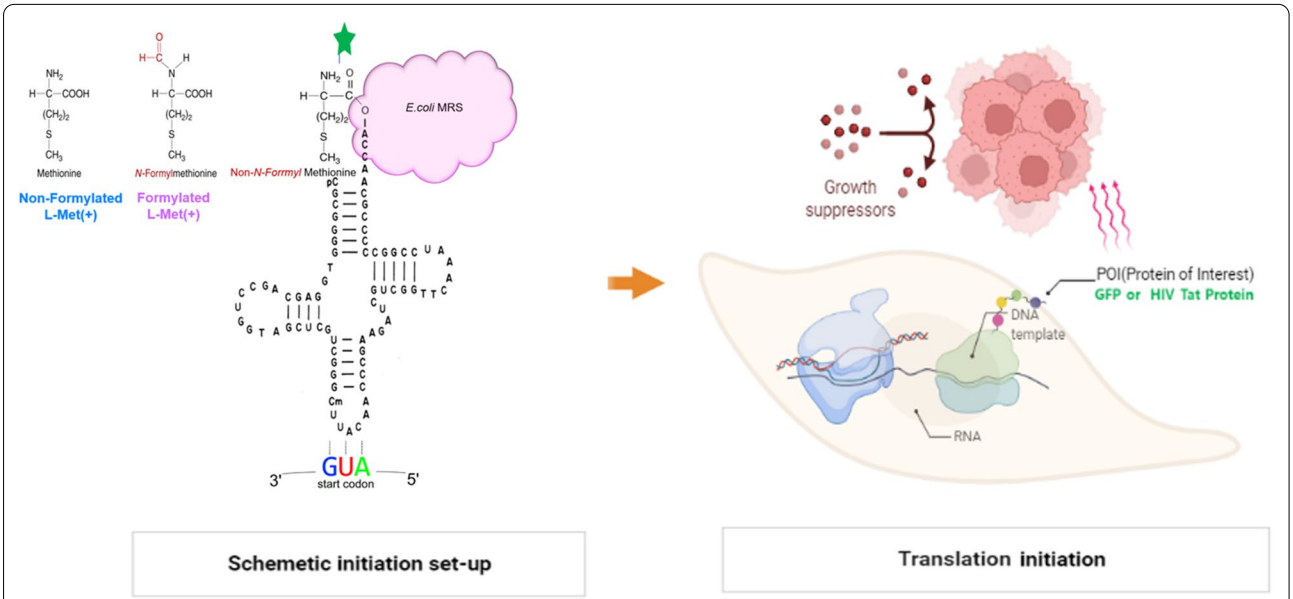

Fig. 1 Schematic depiction of the maintenance of the reading frame for the translational initiation of non-formylated methionine *Escherichia coli* initiator tRNA (*E. coli* Met-tRNAi). Structure of single fluorescent methionine *E. coli* initiator tRNA (fluorescent Met-tRNAi), which initiates the expression of proteins of interest (enhanced green fluorescent protein or Tat). First, a non-formylated group was attached to the free amino group of Met-tRNAi. Met-tRNAi was fluorescent-labeled via a reaction with its amine reactive group. Methionylation via *E. coli* methionyl tRNA synthetase (EcMRS) charged *E. coli* Met-tRNAi for incorporation into the proteins of interest in HeLa cells

SEC–high-performance liquid chromatography-fluorescence detection (SEC-HPLC). The analysis of fluorescent-labeled methionine was purified by reverse phase chromatography using a C18 column (4.6 × 250 mm) on an Agilent HPLC system. Analysis of purification by reverse-phase chromatography showed that the solvent system consisted of solvent A (0.1% trifluoroacetic acid (TFA), 99.5% purity) (Sigma-Aldrich) and solvent B (0.1% TFA in acetonitrile), and was linear against solvent B, with a gradient of 20–100% and a flow rate of 1 mL/min. Purity was confirmed to be > 95%.

Cell culture and enhanced green fluorescent protein (EGFP) transfection *via* methionine presence in media

MEM medium without phenol red (Welgene Inc., Daegu, South Korea) was cultured in HeLa cells, supplemented with 10% fetal bovine serum (v/v) and 1% penicillin/streptomycin (v/v) in 5% CO_2 at 37 °C. The cells were transfected with 2 µL of Lipofectamine 2000 (Invitrogen, Carlsbad, CA, USA) at 60–90% confluence using 500 ng plasmid per 2×10^6 cells. The grown cell medium was washed twice with 1 × phosphate buffered saline (PBS) at pH 7.4, and once more with 1 × PBS (pH 7.4). For EGFP expression, a change to methionine-free MEM (without phenol red) was performed before 3–6 h co-transfections (Welgene Inc., Daegu, Republic of Korea) [39, 40] of EGFP plasmid. *E. coli* initiator tRNA (< 100 pmol per 2×10^6 cells), plus L-methionine, were performed using Lipofectamine 2000, at 37 °C, for 24 h (Fig. 4). HeLa cells were co-transfected with EGFP plasmid and 5-FAM-labeled methionine *E. coli* initiator tRNA using Lipofectamine 2000. Briefly, the expression of 5-FAM-labeled nascent proteins with initiator tRNA, involved the co-transfection of a mixture of EGFP plasmid and 5-FAM-labeled methionine *E. coli* initiator tRNA, were co-transfected using Lipofectamine 2000 at 37 °C for 24 h.

Construction of expression plasmid (EGFP)

An EGFP gene (720 nucleotide pairs) was obtained by the PCR amplification of a pEGFP-N1 vector (Takara Bio, Ann Arbor, MI, USA) using the following PCR conditions: 95 °C for 10 min, 25 cycles at 94 °C for 1 min, 50 °C for 1 min, 72 °C for 2 min, followed by 72 °C for 5 min.

The forward primer was 5'-GGCACAAGCTGG AGTACAAC-3' and the reverse primer was 5'-ATG CCGTTCTTCTGCTTGTC-3'. The PCR product was then cloned into pcDNA3.1 + (Invitrogen), at the KpnI and SalI sites, using the standard restriction cloning methods.

Flow cytometry for determination of *E. coli* initiator tRNA activity

The level of EGFP expression was assessed in two different growth stages, namely the logarithmic and stationary stages. EGFP expressed in HeLa cells was harvested by trypsinization, centrifuged at 3000 rpm for 15 min, washed, resuspended at 10^6 cells/ml in PBS, and stored on ice. Harvested EGFP cells were analyzed on a FACSCalibur flow cytometer (Becton Dickinson, Franklin Lakes, NJ, USA) equipped with a 15 mV, 488 nm, air-cooled argon ion laser. The FACS caliber flow cytometry results recorded 50,000 events, and EGFP expression was assessed in Met^- or Met^+ medium. The EGFP fluorescence of each cell was identified and calculated using standard optics. Color compensation was performed to eliminate artifacts due to the overlap of EGFP fluorescence. Analysis of EGFP overexpression was performed using laser-induced fluorescence and a BD FACSVerse flow cytometer. The flow cytometry histograms of EGFP protein expression were determined using EGFP fluorescence. EGFP fluorescence obtained images by flow cytometry were normalized to the same intensity range, with an acquisition time of 2.5 s. Flow cytometric analysis was performed using BD FACSuite software and Flow Jo (Becton, Dickinson & Company, Franklin Lakes, NJ, USA).

qRT-PCR

Total HeLa cell RNA for qRT-PCR was extracted using RNeasy Mini Kits (Qiagen) according to the manufacturer's instructions. Total RNA (0.15 µg) was used to prepare single-stranded cDNA, using Superscript III Reverse Transcriptase (Invitrogen) and an oligo dT primer. Real-time qPCR was performed using 15 ng of cDNA, SYBR Green (LightCycler® 480 SYBR Green I Master), and LightCycler PCR equipment (Roche Diagnostics, Basel, Switzerland). The PCR conditions were as follows: 95 °C for 5 min, followed by 40 cycles of 10 s at 95 °C for 15 s, 56 °C, and 72 °C for 20 s. The EGFP forward primer was 5'-GGCACAAGCTGGAGTACAAC-3' and the reverse primer was 5'-ATGCCGTTCTTCTGCTTGTC-3'. All measurements were normalized to GAPDH.

Mass analysis of the modified initiator tRNA

Fluorescent-labeled methionine was purified using human Met-tRNA synthetase preparations. After incubation at 37 °C for 10 min, 0.1 volume (2.5 M) (pH 4.5) was added to the reaction mixture. The tRNA was then extracted with phenol saturated with 10 mM NaOAc (pH 4.5), ethanol precipitated, and centrifuged. The fluorescent-labeled methionine initiator tRNA pellet was dissolved in RNase-free water. The in vitro transcription

of fluorescent methionine human initiator tRNA via T7 RNA polymerase human initiator tRNA (73 bp) was detected by agarose gel separation and MALDI-TOF/TOF 5800 (AB Sciex, Toronto, Canada) in the linear and positive ion modes [41]. For all experiments, the matrix solution consisted of 3-hydroxypicolinic acid (50 g/L in H_2O) and diammonium citrate (50 g/L in H_2O). With external calibration using sinapinic acid for BSA, the mass accuracy was estimated to be approximately 0 + 1%, or 25 kDa, for tRNAs of this size. An internal calibration was performed.

Fluorescent and biotin labeling Tat protein detection

Tat protein was produced via in vitro translation, complexed with fluorescent-methionine-*E. coli* initiator tRNA, separated by SDS-PAGE, and identified by staining with Coomassie blue (lower panel). The amount of fluorescent Tat protein expression was separated by SDS-PAGE and visualized. For the freeze–thaw lysis of mammalian cells, HeLa cells were plated on 6-cm dishes (2×10^4/dish) (Nalge Nunc, Rochester, NY, USA) and lysed with FT LYSIS Buffer containing 600 mM KCl, 20 mM Tris–Cl (pH 7.8), and 20% glycerol. The HeLa lysate was centrifuged at 15,000 rpm at 4 °C for 15 min, and the clarified supernatant was then loaded onto His-Pur™ Ni–NTA Spin Columns (Pierce Biotechnology, Rockford, IL, USA). The composition of the binding and elution reactions was 50 mM sodium phosphate and 300 mM sodium chloride (PBS) without 10 mM imidazole at pH 7.2 and pH 5.8, respectively. The fluorescent-labeled Tat was separated by SDS-PAGE and stained with Coomassie Blue. Fluorescence image analysis of fluorescent biotinylated Tat expression was conducted using an inverted fluorescence microscope (IX71; Olympus, Japan) (10 × magnification). The fluorescence images were normalized to the same intensity range: 488 nm and 545 nm laser lines were used for the green filter. The laser was focused on the channel using a 20 × objective lens. The fluorescence signals were collected using the same lens and were optically filtered. Green filter set U-MWIBA3 EGFP shift-free (BP460-495 BA510-550) was used to detect green fluorescence.

Cell viability assay

The HeLa cell lines viability status was determimned using a D-Plus™ CCK cell viability assay kit (Dongin LS, Seoul, Korea) in accordance with the manufacturer's protocol. HeLa cells were seeded in 96-well plates that contained 100 µl of 3×10^3 cells/well. After the seeded cells had been cultured for 24 h at 37 °C, the maintained MEM medium was changed between methionine—MEM (without phenol red) and Methionine + MEM (without phenol red) (Welgene Inc., Daegu, South Korea), respectively.

To assess toxicity following *E. coli* initiator tRNA treatment, the cells were treated with diluent concentrations (0,1,5 and 10 nM) of *E. coli* initiator tRNA from *E. coli* initiator tRNA (10 µM/mL) for 24 h.

Following culturing the cells (1×10^4 cells per ml) for 24 h, the methionine-free MEM- or methionine-treated MEM was added with 100 µL of CCK working solution to each well, and the pate contained cells were further incubated for 4 h at 37 °C. The absorbance was measured at 450 nm using a SpectraMax i3 Multi-Mode Platform Microplate Detection (Molecular Devices, LLC, Sunnyvale, CA, USA). The OD value of control cells was considered to represent 100% viability[42].

Statistical analysis

All values are expressed as means. Error bars indicate the standard deviation. Graph Adobe CS7 software was used for graphing and statistical analysis.

Results

Engineering-based synthesis of fluorescent-labeled non-formylated methionine-conjugated *E. coli* initiator tRNA (Met-tRNAi) and protein translation

Figure 1 displays the non-formylated methionine process for protein synthesis in eukaryotic cells using *E. coli* Met-tRNAi. First, we engineered and heterologously expressed fMet-tRNAi, wherein two types of *E. coli* Met-tRNAi were introduced: *E. coli* Met-tRNAi/EcMRS and *E. coli* Met-tRNAi/human methionyl tRNA synthetase (HMRS). We compared the activity of human Met-tRNAi and *E. coli* Met-tRNAi by monitoring the expression of PII such as green fluorescent protein (GFP) or fluorescent N-term-labeled HIV transcription activator protein (Tat) as PII model proteins. Human Met-tRNAi was used as a positive control for the fluorescence-labeled *E. coli* Met-tRNAi-transfected cells (Fig. 1). Codons and amino acids were then assigned to individual tRNAs through selective aminoacylation of the tRNAs using aminoacyl tRNA synthetases [43]. Additional file 1: Fig. S1 [42, 43] shows that tRNAs have a cloverleaf structure and contain all invariant and semi-invariant sequences in both prokaryotic and eukaryotic initiators [44–47].

The preservation of the sequence in eukaryotic tRNAis is a unique property of tRNAi (Additional file 1: Fig. S1A). The unique characteristics of prokaryotic tRNAi may explain the strong conservation of the Watson–Crick base pair at the end of the receptor stem and the presence of the 11-purine:24-pyrimidine base pair (instead of the 11-pyrimidine:24-purine base pair) (Additional file 1: Fig. S1). Three consecutive GC pairs, including sequences

of three guanines and three cysteines, were formed in the anticodon stem in both prokaryotic and eukaryotic tRNAis (Table 1). The schematic in Fig. 1 summarizes the experiment and compares the activity of human and *E. coli* tRNAis during the initiation of PII synthesis in mammalian cells.

Verification of the quality of single fluorescent methionine-conjugated *E. coli* initiator tRNAs

We assessed *E. coli* fluorescent Met-tRNAi, using the size-exclusion chromatography (SEC) method to separate unlabeled methionine-conjugated *E. coli* tRNAi and 5-FAM or methionine (Fig. 2A). The peaks shown on the left of Fig. 2A represent free methionine (210 nm, 13 min), the fluorescent label alone (210 nm, 12 min), and the fluorescence detector (FLD). We previously reported the N-terminal labeling of target proteins with the strong chromophore Cy5-Met [48–51]. Purified Cy5-Met was chemically synthesized and then purified to validate the occurrence of protein synthesis mediated by single *E. coli* fluorescent Met-tRNAi.

We also chemically synthesized 5-FAM-Met, which was then coupled to synthetic *E. coli* tRNAi, as demonstrated by magnetic resonance spectroscopy. *E. coli* tRNAi was generated via in vitro transcription and separated according to mass from 5-FAM (473.39 Da), *E. coli* tRNAi (26.07 kDa), and methionine alone (149 Da) (Fig. 2A). Here, 5-FAM-labeled methionine-charged *E. coli* tRNAi clearly overlaid the fluorescence detection spectra and could be distinguished by its absorbance peak of 210 nm at 5.3 min (Fig. 2B) and a peak at 260 nm at 5.3 min.

The peak corresponding to 5.3 min was further analyzed via matrix-assisted laser desorption ionization time-of-flight mass spectrometry (Fig. 2C and Additional file 1: Fig. S2). As an additional control, we compared the methionylation of fluorescent methionine-conjugated human tRNAi with fluorescent methionine-conjugated *E. coli* $tRNA_i$ using 2% agarose gel electrophoresis, followed by imaging with 260-nm UV irradiation and an FLD (Additional file 1: Fig. S3). To study the effect of the non-formylated methionine-conjugated *E. coli* tRNAi on translation recognition in HeLa cells, we purified EcMRS based on its affinity for *E. coli* fluorescent Met-tRNAi. This enzyme is activated by the amine group of unpurified fluorescent methionine, indicating that non-formylated, rather than formylated, methionine is charged by EcMRS. The effect on a single fluorescent methionine-binding *E. coli* tRNAi was measured for fluorescently labeled synthetic proteins using *E. coli* Met-tRNAi/EcMRS.

The fluorescent methionine-conjugated *E. coli* initiator tRNA mediates the expression of Tat proteins in HeLa cells

To evaluate whether *E. coli* Met-tRNAi conjugated with the N-terminal fluorophore 5-FAM (Ex: 492 nm; Em: 512 nm), HeLa cells were extracted from the C-terminal interaction partner fused to the AVI-Tagged Tat protein to confirm fluorescent Tat expression (Fig. 2D). To verify the translation efficiency of the fluorescence-labeled protein using *E. coli* Met-tRNAi/EcMRS pairs, we prepared a single fluorescent methionine-conjugated *E. coli* tRNAi with an optimized N-terminal recognition motif, and the C-terminal interaction partner was fused to AviTag. Fluorescent protein imaging was performed using biotin double-labeled Tat on polyethylene streptavidin-coated quartz slides.

Additional file 1: Fig. S4 presents gel images of the fluorescence-labeled *E. coli* Met-tRNAi-mediated N-terminal labeling of Tat proteins. To assess *E. coli* tRNAi, we investigated whether the fluorescent *E. coli* Met-tRNAi was involved in the translation of the reading frame using the Tat protein, a factor essential for the transcription of the HIV-1 genome.

Fluorescent-labeled human tRNAi charged endogenous human MRS (lane 2) and *E. coli* tRNAi charged

(See figure on next page.)

Fig. 2 Validation and spectral separation of single fluorescent non-formylated methionine-conjugated initiator tRNA (Met-tRNAi) and production of fluorescent biotin-labeled Tat proteins using non-formyl methionine *Escherichia coli* initiator tRNA (*E. coli* Met-tRNAi) and *E. coli* methionyl tRNA synthetase (EcMRS) in HeLa cells. **A** Chromatogram spectra for unlabeled *E. coli* initiator tRNA (tRNAi), L-methionine, and 5-carboxyfluorescein (excitation, 492 nm; emission, 517 nm) resolved using size exclusion high-performance liquid chromatography (SEC-HPLC). Major peaks indicate ultraviolet light alteration (UV; 210 nm). The positive control, *E. coli* tRNAi, and human tRNAi are shown in black (UV; 260 nm). **B** The highest peak corresponds to fluorescent Met-tRNAi (UV 210 nm; red line, UV 260 nm; black line, fluorescence detection [FLD]; blue line). The positive control with tRNAi (UV; 260 nm) was used to verify the quality of the fluorescent Met-tRNAi shown in black (UV; 210 nm, FLD; excitation, 492 nm; emission, 517 nm). **C** Comparison of *E. coli* tRNAi (green line in 2C) and *E. coli* fluorescent Met-tRNAi (blue) using matrix-assisted laser desorption ionization time-of-flight mass spectrometry. **D** The activity of the sequence/structure and cellular endogenous human tRNAis activity of the sequence/structure in mammalian cells compared with that in *E. coli* tRNAis. The orthogonality of replacing endogenous human tRNAi with *E. coli* tRNAi in association with human methionyl tRNA synthetase (HMRS) and EcMRS-mediated fluorescent biotinylated Tat expression was analyzed using immobilized quartz slides coated with streptavidin. Image of fluorescent biotinylated Tat shows binding of EcMRS to *E. coli* tRNAi. The *E. coli* Met-tRNAi/EcMRS pairs and *E. coli* Met-tRNAi/HMRS pairs were confirmed using fluorescent Tat expression (excitation, 492 nm; fluorescent emission of Tat, 517 nm)

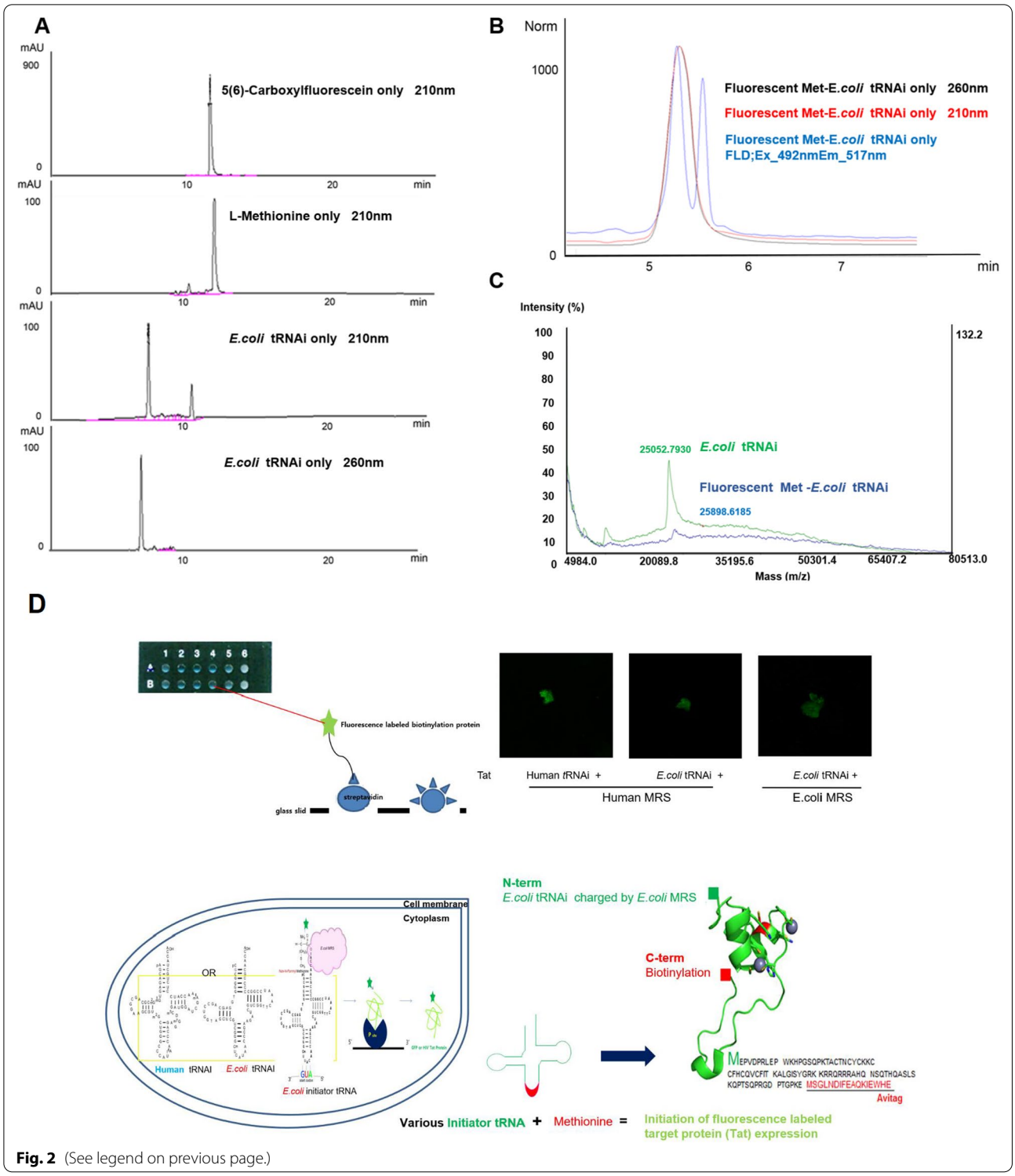

Fig. 2 (See legend on previous page.)

EcMRS (lanes 3, 4, and 5), identified via Tat expression as a positive control (17 kDa), were analyzed through fluorescence scanning and SDS-PAGE (Additional file 1: Fig. S4). The results show that *E. coli* Met-tRNAi/EcMRS pairs migrated in a fluorescent band pattern with fluorescent-labeled Tat protein expression as the positive control. One of the two suggested hypotheses was that the *E. coli* Met-tRNAi/HMRS pair with the fluorescent band

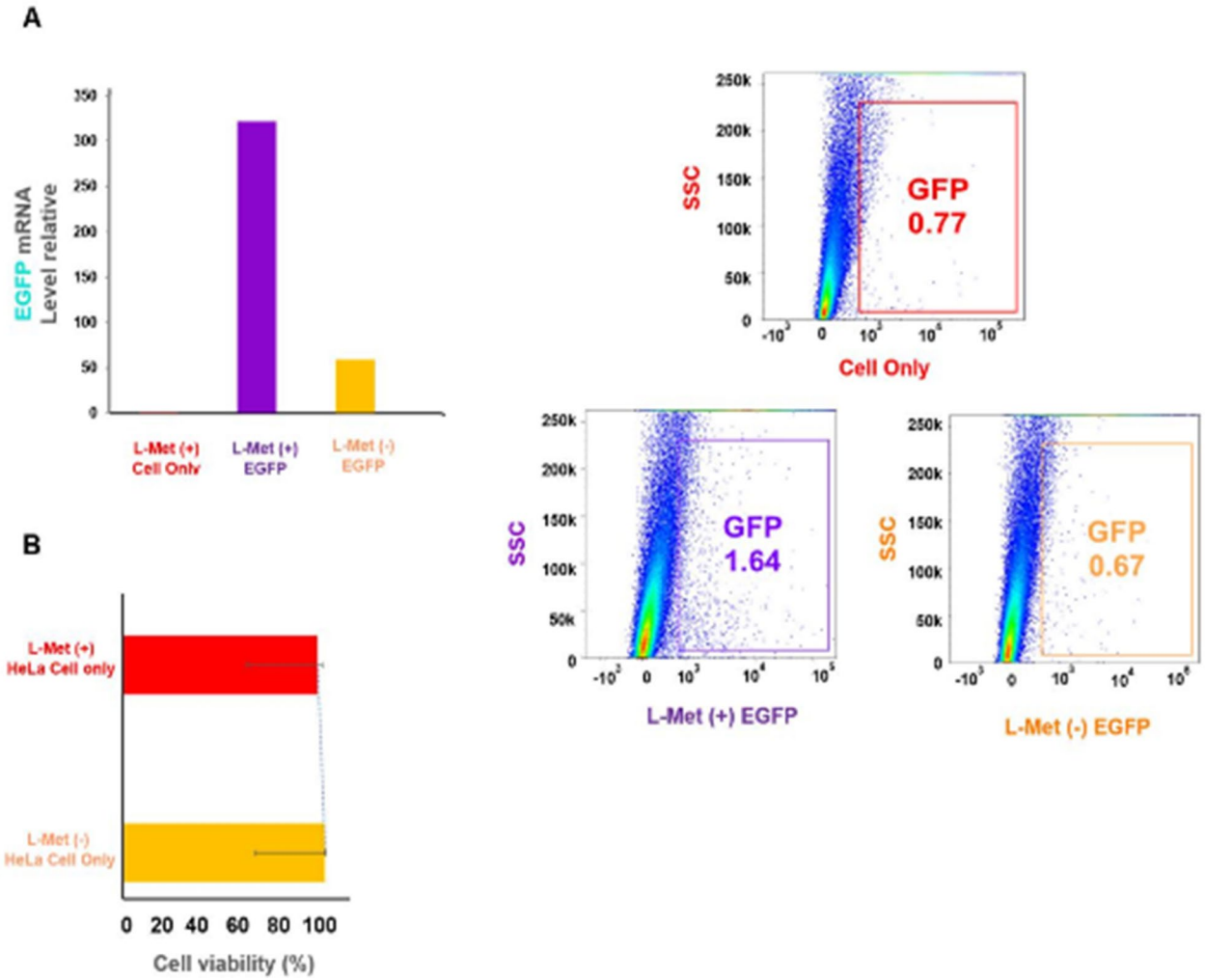

Fig. 3 Introduction of enhanced green fluorescent protein (EGFP) mRNA expression in methionine-deficient medium to evaluate HeLa cell viability. **A** EGFP mRNA levels were quantified using quantitative real-time polymerase chain reaction (qRT-PCR) and normalized to GAPDH from endogenous human initiator tRNA (dark violet) in HeLa cells. Samples of EGFP-positive cells in an L-methionine (L-Met)–deficient medium (orange), HeLa cells only (red), and endogenous human RNAi were expressed in methionine-positive HeLa cells (dark violet). The EGFP expression levels are shown as the relative fluorescence populations in the dot plots. A flow cytometry analysis was conducted using EGFP cells in the absence or presence of L-Met, as follows: HeLa cells only (red), L-Met positive media (dark violet), and human initiator tRNA in an L-Met-free medium (orange). All data obtained in the FACS and qRT-PCR experiments are expressed as the mean ± standard deviation of three independent experiments. **B** Effect of L-Met on HeLa cell viability. HeLa cells were treated with L-Met (red bar) or without L-Met (orange bar) for 24 h. Cell viability was determined using CCK8 assays and calculated relative to that of the control HeLa cells (L-Met sufficiency). Data are presented as the mean ± standard error of the mean (SEM) for three independent experiments

would result in Tat identification as a 17-kDa band when expressed Tat was dyed with Coomassie brilliant blue staining solution (lane 1 and 2 in Additional file 1: Fig. S4). HMRS and EcMRS utilization led to the identification of mRNAs involved in Tat expression (Figs. 3 and 4). In contrast, the efficiency of protein initiation synthesis by fluorescent-Met-tRNAi/EcMRS was not well detected because of the disruption of endogenous protein expression in the Coomassie-stained gel.

Our results show that *E. coli* Met-tRNAi enables target protein synthesis in live HeLa cells and allows visualization of the proteins in the fluorescent imaging molecules in response to protein translation mediated by tRNAi/MRS pairs. In addition, fluorescence-tagged Tat protein expression occurred simultaneously with Tat protein expression based on tRNAi translation. Various results for the fluorescent *E. coli* Met-tRNAi strategy mediated PII synthesis are presented in Table 2.

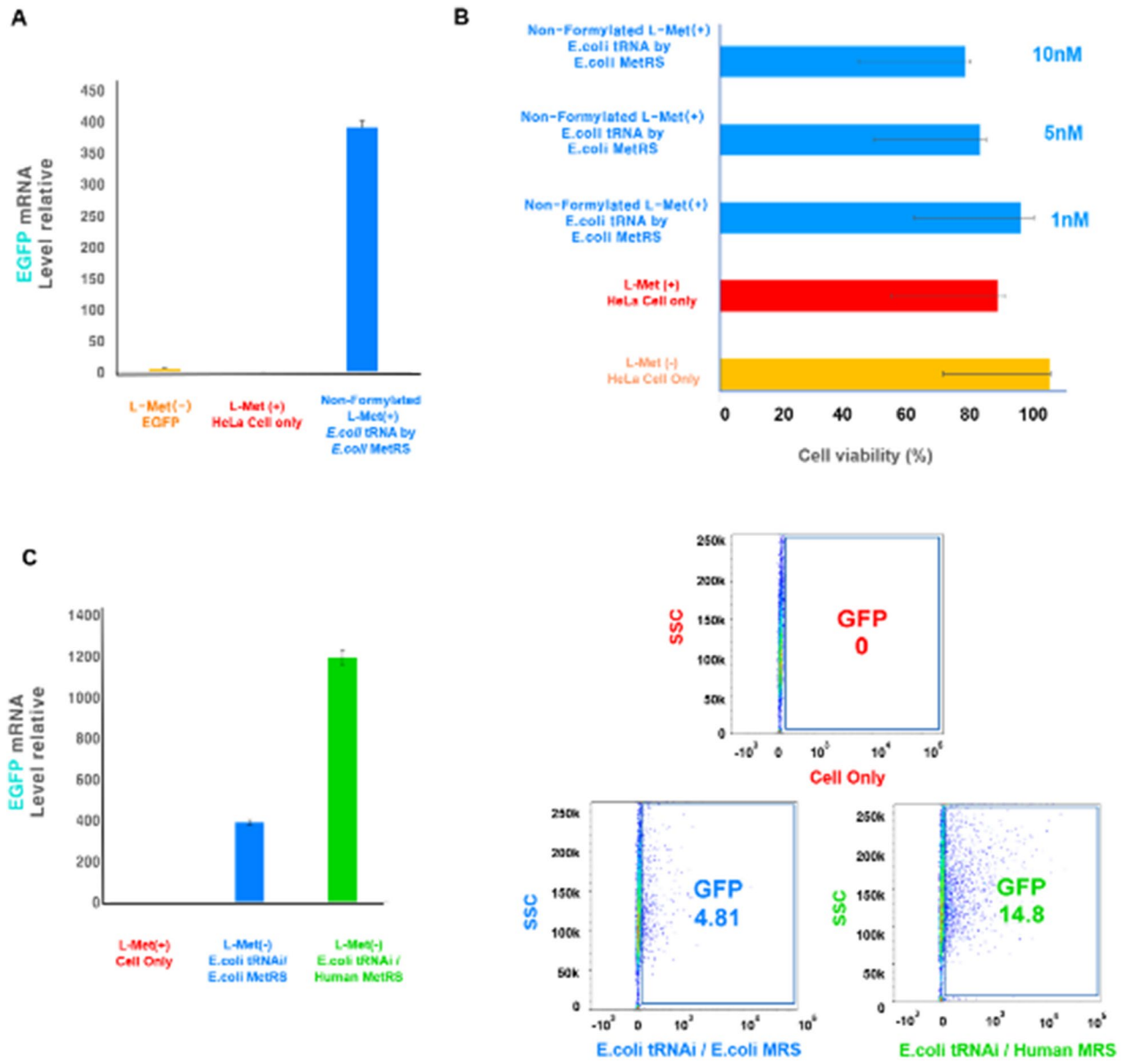

Fig. 4 Comparison of enhanced green fluorescent protein (EGFP) mRNA expression following the initiation of the translational reading frame induced using non-formyl methionine *Escherichia coli* initiator tRNA (Met-tRNAi) from *E. coli* methionyl tRNA synthetase (EcMRS) and human methionyl tRNA synthetase (HMRS). **A** EGFP mRNA levels were quantified using quantitative real-time polymerase chain reaction (qRT-PCR) and normalized to GAPDH in the presence of *E. coli* Met-tRNAi/EcMRS pairs (blue bar) in HeLa cells. **B** Effect of *E. coli* Met-tRNAi with EcMRS on HeLa cell viability. Cell survival was measured using cell assays with specific concentrations (1, 5, and 10 nM) of *E. coli* Met-tRNAi/EcMRS pairs (blue bars). The effect of non-formylated L-methionine (L-Met) on HeLa cell viability was determined via qRT-PCR analysis of EGFP mRNA expression. HeLa cells were treated with (red bar) or without L-Met (orange bar) for 24 h. Cell viability was determined using CCK8 assays and calculated relative to that of the control HeLa cells (red bar). Data are presented as the mean ± SEM of three independent experiments. **(C)** qRT-PCR (right) and dot plots showing EGFP expression (left). HeLa cells were treated with *E. coli* Met-tRNAi/HMRS (green bar) for 24 h. The qRT-PCR results were normalized to GAPDH. Bars represent the mean ± standard deviation of three independent experiments. Dot plots for EGFP expression in a L-Met-free medium (orange line), HeLa cells only (red line), *E. coli* Met-tRNAi/EcMRS pairs (blue line) and *E. coli* Met-tRNAi/HMRS pairs (green line) are shown

As shown in Fig. 2, fluorescent methionine was chemically synthesized and then purified to confirm the occurrence of protein synthesis [40, 52, 53]. We introduced fluorescence-labeled Tat protein with non-purified fluorescence-labeled Met-conjugated human tRNAi to HeLa lysates. To demonstrate further the

Table 1 Structural comparison of human initiator tRNAs and *Escherichia coli* initiator tRNAs

Classification	Human initiator tRNA (73 nt , 24.910 kDa)[a]	*E.coli* initiator tRNA (76 nt , 26.097 kDa)[b]
LOOP I Dihydrouridine loop	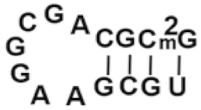	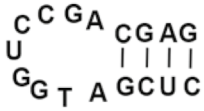
LOOP II Anticodon loop		
LOOP III variable loop	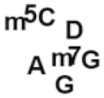	
LOOP IV T ψ C loop		
Acceptor stem	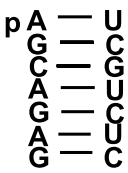	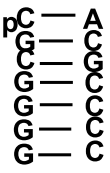

[a] Adapted from Drabkin et al. [15]

[b] Adapted from Seong. et al. [16]

evaluation of this approach, the non-purified fluorescent Tat protein obtained through sodium dodecyl-sulfate polyacrylamide gel electrophoresis (SDS-PAGE), we examined the fluorescent Tat, which was double-tagged with biotin, on streptavidin-coated slides. The initiation of protein synthesis suggested that tRNAis can become novel regulators that maintain the translational reading frame.

Therefore, the results of this study provide new insights into the optimization of initiation tRNAi motifs to allow control over the initiation of protein synthesis. Moreover, our observations of the fluorophore-*E. coli* Met-tRNAi bases further advance the understanding of protein expression in eukaryotic cells by revealing the various initiating tRNA sequence motifs involved in protein synthesis and fidelity. Therefore, the results of this study provide new insights into the roles of various tRNAis in protein fidelity and could be used to develop a strategy for the optimization of initiation tRNAi motifs to facilitate precise protein synthesis.

Validation of an *E. coli* Met-tRNAi HeLa cell platform in a methionine-deficient medium

We validated Tat expression using a fluorescence-labeled, methionine-conjugated human tRNAi probe (Fig. 1). As previously reported, EGFP expression was measured in an L-Met–deficient medium, demonstrating the translational recognition of human Met-tRNAi-mediated selective protein expression in HeLa cells [38, 40]. In the Met-sufficient growth medium, cells were cultured with

Table 2 tRNA-mediated fluorescent labeling expression system in published during 2005–2022

Host cell	Fluorophore-conjugated tRNA species	Reference
E.coli	suppressor tRNA	JIŘÍ Koubek et al. [64]
E.coli	V-Spinach tRNA	Isao Masuda et al. [65]
E.coli /human cells/cell free system	orthogonal tRNA(chemically engineered tRNA)	Naohiro Terasaka et al. [66]
		Robert B. Quast et al. [67]
		Lena Thoring et al. [68]
E.coli	*E.coli* initiator tRNA	Jun et al. [37]
E.coli	Suppressor *E.coli* initiator tRNA	Miura et al. [48]
Chinese hamster ovary cells (CHO)	total yeast or bovine tRNA	Sima Barhoom et al. [69]
Human tissue cells	Human tRNA	Kimberly A Dittmar et al. [70]
Human cells	Human initiator tRNA	Kim et al. [40]
HeLa cells	*E.coli* initiator tRNA	This study

the other 19 natural amino acids, while fluorescence-labeled methionine was added to the cells during the stationary growth phase. To initiate *E. coli* Met-tRNAi-mediated selective protein synthesis, we co-transfected an EGFP-expressing plasmid with human Met-tRNAi into HeLa cells. As shown in Fig. 3A, EGFP-expressing cells exhibited lower levels of EGFP mRNA, and EGFP expression was reduced in both methionine-free and -sufficient cells.

EGFP mRNA levels were determined using quantitative real-time polymerase chain reaction (qRT-PCR) and were correlated with green fluorescence (Fig. 3A, left). Despite the presence of low levels of endogenous tRNAi in the L-Met–free medium, which indicates low levels of EGFP expression, this strategy was found to be applicable to the use of *E. coli* tRNAi as the positive control (Fig. 3A). The flow cytometry results indicated that EGFP expression gradually increased in the methionine-supplemented medium, as did the level of EGFP. As shown in Fig. 3 (right and left panels), the analysis of EGFP via flow cytometry following incubation in Met-deficient media indicated that EGFP was highly expressed in Met-supplemented media (GFP population 1.64, dark violet), while there was a clear quantitative separation of EGFP mRNA expressed in Met-deficient medium (GFP population 0.67, orange).

Flow cytometry dot plots of EGFP expression in methionine-free cell lines expressing EGFP were also analyzed to confirm consistency with the EGFP mRNA levels. The level of green emission observed from EGFP-expressing cells was approximately two-fold higher (GFP population 1.64, dark violet) than that from methionine-free HeLa cells (GFP population 0.67, orange; Fig. 3A). Based on these results, *E. coli* Met-tRNAi can be used for protein synthesis in methionine-free cells. The expression of GFP mRNA increased after the introduction of EGFP-transfected HeLa cells, but L-Met deficiency and L-Met sufficiency acted as positive controls in correlation with HeLa cell viability (Fig. 3B). Thus, the effect of L-Met on HeLa cell viability occurs during initial translation. The decrease in the viability of HeLa cells without methionine was not significant compared with that of control HeLa cells with sufficient methionine (Fig. 3B). This result provides experimental proof of the Hoffman effect [54], whereby malignant cells can endogenously synthesize high levels of methionine, which is insufficient to sustain cancer growth. Human tumor cells have been reported to depend on exogenous methionine, whereas normal tissue may depend on homocysteine to meet methionine needs [55, 56]. This means that malignant cells can adapt to glucose-poor conditions by adopting alternative metabolic pathways that support growth [57–59]. Therefore, by introducing our methionine-deficient medium condition, the viability characteristics of methionine-dependent HeLa cells were efficiently applied to the experimental system to illustrate the significance of *E. coli* tRNAi-mediated initiation protein synthesis and previous reports [55, 56].

EGFP expression *via* the initiation of the translational reading frame with *E. coli* Met-tRNAi/ EcMRS pairs

To evaluate the activity of *E. coli* tRNAi, EGFP was expressed by transfecting HeLa cells in a L-Met–free medium. The *E. coli* Met-tRNAi/EcMRS-charged *E. coli* tRNAi, which was used as a bio-orthogonal reaction, was paired with proteins produced in eukaryotic hosts (Fig. 4A). The EGFP mRNA levels determined through qRT-PCR demonstrated a correlation with the *E. coli* Met-tRNAi/EcMRS pairs. In the experiment involving *E. coli* Met-tRNAi/EcMRS pairs alone, EGFP mRNA expression (blue bars), EGFP expression dot plots (Additional file 1: Fig. S4, GFP group 0.58, blue), and EGFP

mRNA expression induced with L-Met were observed in the methionine-deficient medium (Fig. 4A; GFP population 0.35, orange). In addition, EGFP mRNA expression was observed after introducing *E. coli* Met-tRNAi/EcMRS pairs alone with L-Met–sufficient HeLa cells used as a control (Fig. S4: GFP population 0.01, red). Figure 4B shows that HeLa cell viability was induced by GFP mRNA expression. In HeLa cells without methionine, cell viability, which was introduced by adding 1, 5, and 10 nM of the *E. coli* Met-tRNAi/EcMRS pair (blue bar), was dependent on the concentration change of the HeLa cell control with sufficient methionine. The *E. coli* Met-tRNAi/EcMRS pair showed significant toxicity at a concentration of 10 nM, as shown in Fig. 4B.

The results suggest the possibility of an association with the GFP mRNA expression level introduced by the *E. coli* Met-tRNAi/EcMRS pair (blue bar) shown in Fig. 4A. As shown in Fig. 4, the expression of GFP mRNA decreased after the introduction of the *E. coli* Met-tRNAi/HMRS pair (green bar), unlike that in the *E. coli* Met-tRNAi/*Ec*MRS (blue bar) pair comparison experiment. The expression of GFP mRNA increased after introducing the *E. coli* Met-tRNAi/HMRS pairs (green bars), as shown in Fig. 4C. The expression of *E. coli* Met-tRNAi/HMRS pairs was higher under methionine-deficient HeLa cell conditions than that observed when using *E. coli* Met-tRNAi/*Ec*MRS pairs (Fig. 4C, GFP population 14.8, green). Furthermore, the expression of GFP mRNA decreased after introducing the *E. coli* MRS pair. The results for the HMRS group were compared with that of the introduction of an *E. coli* initiator charged with EcMRS (Fig. 4C; GFP population 4.81, blue) as a replacement for HMRS (Fig. 4C, GFP population 14.8, green). We found that the expression of GFP mRNA increased after the introduction of EGFP expression.

By comparing the results obtained for MRS substitution, we found that MRS from humans and *E. coli* synthesized PIIs in the cytoplasm. These results indicate that various tRNAis potentially act on different tRNA sequence motif interactions.

These results suggest that introducing *E. coli* Met-tRNAi/EcMRS pairs in the initial translation frame for GFP mRNA expression inhibits protein initiation due to cytotoxicity.

Comparison of the effect of formylated methionine-conjugated and non-formylated methionine-conjugated *E. coli* tRNAi on the survival of HeLa cells

Next, to determine the viability of *E. coli* tRNAi in non-formylated methionine used in the initial translational reading frame, samples with non-formylated and formylated methionine were compared by monitoring the viability of HeLa cells. In methionine-free HeLa cells, non-formylated methionine-conjugated *E. coli* Met-tRNAi/EcMRS pairs (1, 5, and 10 nM) exhibited a significantly higher level of toxicity compared with that seen in formylated methionine-conjugated *E. coli* Met-tRNAi/HMRS pairs (Fig. 5 and Additional file 1: Figs. S5 and S6). Non-formylated methionine bound to *E. coli* tRNAi was associated with lower cell viability than formylated methionine bound to *E. coli* tRNAi.

In the absence of the introduction of protein initiation, the HeLa cell viability results suggest that methionine is a complex metabolic pathway that is associated with cancer at multiple levels. However, the lower HeLa cell viability observed when non-formylated methionine was introduced during the initiation of protein synthesis suggests that the cytotoxicity induced in the early translation frame of GFP mRNA expression is significantly associated with EcMRS. Generally, most cells readily synthesize methionine from homocysteine but cannot proliferate in a medium where methionine has been replaced with homocysteine. Therefore, the results shown in Figs. 5A and 5B suggest that the increased viability of HeLa cells in the methionine-deficient state (orange bars) could mean that HeLa cells replaced methionine with homocysteine [55] are associated with increased HeLa cell viability.

Although the accurate determination of the efficiency of synthesized proteins remains controversial, catalyzing the linking of amino acids to cognate transfer RNAs (tRNAs) could be controlled by inducing the PII expression. We found that the selective linking of a fluorescent methionine to *E. coli* Met-tRNAi was highly precise, as shown in Fig. 5. Moreover, every EcMRS paired with methionine could be promoted as a newly synthesized protein in HeLa cells. Many types of aaRS can be tracked via their pairing with cognate tRNAs to investigate the fidelity of protein translation.

Discussion

We showed that *E. coli* methionine-tRNAi could offset human methionine-tRNAi, and *E. coli* methionine-tRNAi/methionyl tRNA synthetase pairs can drive enhanced GFP mRNA expression. *E. coli* methionine-tRNAi/methionyl tRNA synthetase pairs can induce enhanced green fluorescent protein(GFP) expression due to increased stability of enhanced GFPmRNA. This study investigated various differences in tRNAi species on protein expression by observing POI synthesis in HeLa cells using *E. coli* tRNAi. Although it is common for PII expression to change when tRNAi changes, we evaluated the relationship between mRNA stability and cell viability. The low HeLa cell viability due to non-formylated methionine introduced during protein synthesis

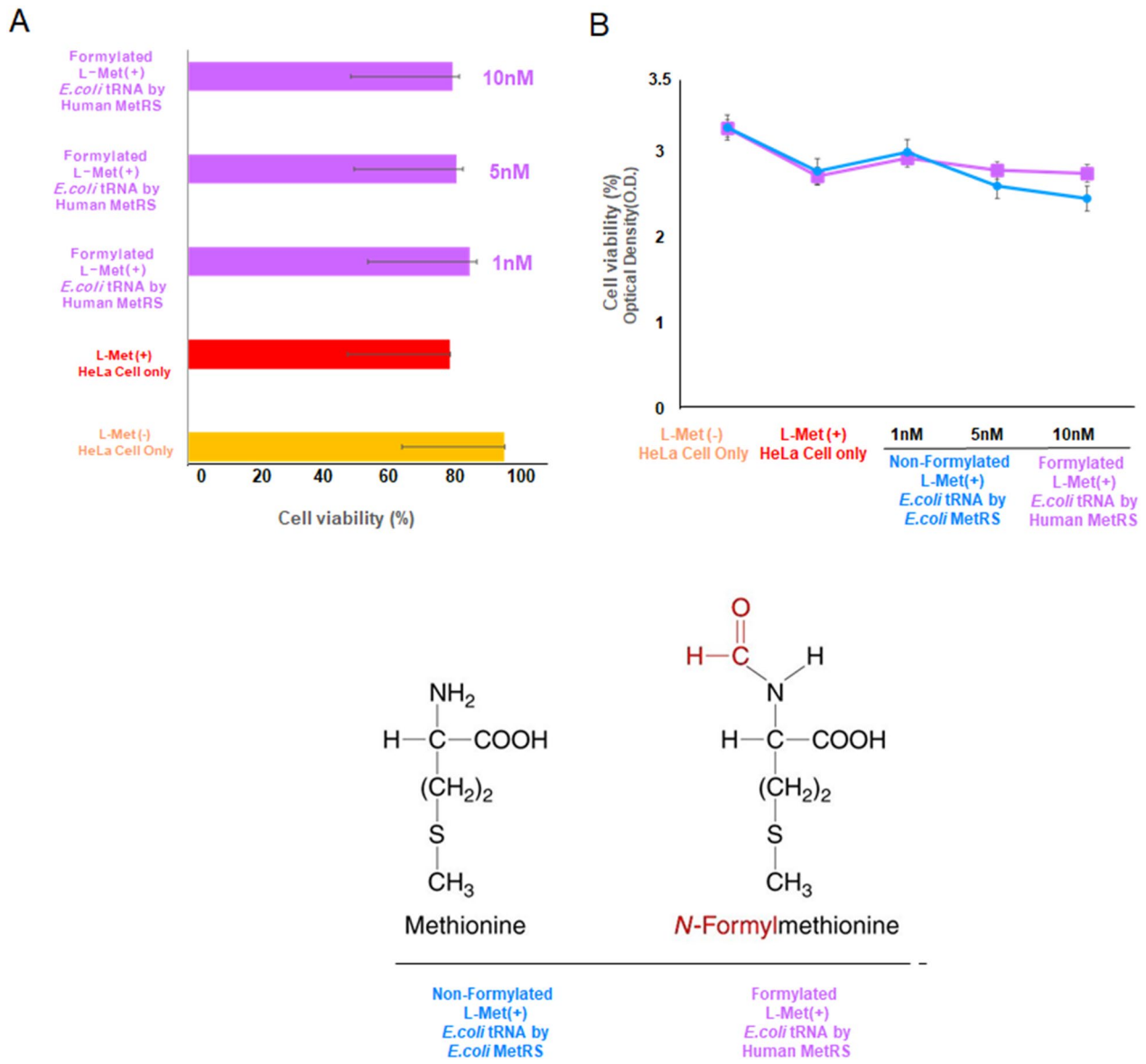

Fig. 5 Comparison of HeLa cell viability using non-formylated methionine-conjugated initiator tRNA (Met-tRNAi) and formylated Met-tRNAi (fMet-tRNAi). **A** Effect of *E. coli* fMet-tRNAi/human methionyl tRNA synthetase (HMRS) on HeLa cell viability. Cell survival was measured using cell assays at specific concentrations (1, 5, and 10 nM) of *E. coli* Met-tRNAi/HMRS (violet bars). **B** Comparison between the effects of formylated L-methionine (L-Met) conditions based on specific concentrations (1, 5, and 10 nM) of *E. coli* tRNAi. The cell viability analysis was conducted on HeLa cells using *E. coli* Met-tRNAi charged with *E. coli* methionyl tRNA synthetase (blue line) and *E. coli* fMet-tRNAi charged with HMRS (violet line). The effect of formylated L-Met on HeLa cell viability was determined via quantitative real-time polymerase chain reaction analysis of enhanced green fluorescent protein mRNA expression. HeLa cells were treated with (red line) or without L-Met (orange line) for 24 h. Cell viability was determined using CCK8 assays and calculated relative to that of the control HeLa cells (red line). Data are presented as the mean ± SEM of three independent experiments

initiation suggests that cytotoxicity induced in the initial translation of GFP mRNA is significantly associated with EcMRS.

However, despite the effect of unlabeled methionine on the fluorescent *E. coli* Met-tRNAi, we were able to implement the necessary conditions to measure biotinylated fluorescent Tat (PII)-expressing proteins using *E. coli* Met-tRNAi/EMRS. Unlike the human methionine-tRNAi/methionyl tRNA synthetase pairs that were used as a positive control, the non-formylated *E. coli* methionine-tRNAi/methionyl tRNA synthetase pairs reduced

the expression of enhanced GFP mRNA, resulting in reduced HeLa cell survival.

In 2017, we reported a PII detection strategy wherein the fluorescent-labeled N-terminal was conjugated with Met-tRNAi (fluorescent Met-tRNAi) to validate the occurrence of protein synthesis [40]. Previously reported in 2017, Purified Cy5-Met (fluorescent Met) was added to the human tRNAi after aminoacylation. Additionally, during synthesis, combining fluorescent Met-tRNAi with a purified Cy5-Met process allowed the translation of the mRNA encoding fluorescent-labeled PII in HeLa cells. In contrast, in this study, fluorophore 5 carboxyfluorescein (5-FAM) was added to *E. coli* Met-tRNAi after aminoacylation. The non-formylated Met-*E. coli* tRNAi/EcMRS pair showed decreased cell proliferation in HeLa cells due to a correlation with low protein synthesis efficiency. As many tRNAs possess unique features, we investigated whether tRNAs are sequestered for the exclusive initiation of protein synthesis or whether they are associated with the role of tRNAis in protein synthesis, as shown in Additional file 1: Fig. S1. It is most likely that one modified nucleotide is present in the tRNA, indicating that the process of maintaining the translational reading frame occurs early in the emergence of new phylogenetic domains [60].

Most tRNA modifications can also have specific functions through which tRNAs participate in the aaRS reaction. Aminoacyl tRNA has a high substrate selectivity and faithful synthesis through the editing of non-cognate products via selective aaRS activity [26]. However, this process can introduce errors in protein synthesis while attaching certain amino acids to non-cognate tRNAs with a high level of accuracy [24]. Therefore, the tRNA sequence motif interaction between synthetase and tRNA is a potential factor that ensures the accuracy of the translational reading frame. Here, we sought to capture the interactions of tRNA during a mRNA stability event.

However, the low level of specificity achieved by misaminoacylation can result in mistranslation, which might be lethal and lead to pathologies in mammalian cells [61]. Although tRNA and aminoacyl tRNA synthesizer (ARS), which are involved in protein translation, are considered "housekeeping" molecules without functional activity [62], ARS is also reportedly involved in various physiological and pathological processes, particularly in tumorigenesis [39, 62, 63].

The methionine-dependent Hoffman effect has also been reported [54] in cancer cells, which rely on exogenous methionine. The Met-tRNAi complex has been proposed to regulate the translation of key genes involved in tumorigenesis because of its unique function in translation initiation, which may indicate the potential of *E. coli* Met-tRNAi/MRS pairs as possible biomarkers to predict clinical outcomes. Although the accurate determination of the efficiency of synthesized proteins remains controversial, catalyzing the linking of amino acids to cognate transfer RNAs (tRNAs) could be controlled by inducing the initiation of the PII expression.

However, this study has some limitations. The correlation between the *E. coli* MettRNAi/EcMRS pair and early cancer cell survival identified here may not be seen in overall cells. Despite the lack of known similar mechanical evidence, important and consistent correlations between *E. coli* Met-tRNAi/EcMRS pairs allow the potential biomarkers and molecular initiation's insights for fine-tuned protein synthesis can the identification of PIIs in the context of mRNA-tRNA pairs.

Abbreviations

tRNAs: Transfer RNAs; EGFP: Enhanced green fluorescent protein; GFP: Green fluorescent protein; FBS: Fetal bovine serum; MEM: Minimum Essential Media; PBS: Phosphate-Buffered Saline; *E. coli*: *Escherichia coli*; MET: Methionine; Met AP: Methionine aminopeptidase.

Supplementary Information

The online version contains supplementary material available at https://doi.org/10.1186/s13765-022-00748-0.

Additional file 1: Fig. S1. Diagram of human and *E. coli* initiator tRNAs. **Fig. S2.** Mass spectra of initiator tRNA. **Fig. S3.** Analysis and visualization of fluorescently labeled methionine-charged *E. coli* initiator tRNA pairs. **Fig. S4.** EGFP expression levels in HeLa cells with a non-formyl methionine-*Escherichia coli* (*E. coli*) initiator tRNA (Met-tRNAi) employing *E. coli* methionyl-tRNA synthetase (EcMRS) counterpart. **Fig. S5.** Quantitative analysis of enhanced green fluorescent protein (EGFP) expression, after treating HeLa cells with non-formylated, Met-charged *E. coli* initiator tRNA.

Acknowledgements

We thank Dr. Baik Lin Seong (Yonsei University) for valuable advice. We also thank Dr. Sang-Hyeon Kang (iNtRON Biotechnology) for *E. coli* tRNA technical supports. The expression vector encoding the human initiator tRNA gene was a gift from Dr. Sung Hun Kim (Yonsei University). We are also grateful to Dr. Joo Hee Chung of the KBSI (Seoul) for HPLC and MALDI TOF analysis.

Author contributions

JMK designed the research and conducted the experiments. JMK and JJH discuss the paper. JMK and HYL conducted the experiments. All authors read and approved the final manuscript.

Funding

This research was supported by Basic Science Research Program through the National Research Foundation of Korea(NRF) funded by the Ministry of Education(2022R1A6A3A01086819)(JMK). This work was also supported by the National Research Foundation of Korea (NRF) grant funded by the Korea government (MSIT) (No.2022-0662) (HYL).

Availability of data and materials

All data discussed in this paper are available in the main text and Supplementary Information. The materials used in this study are available upon request from the corresponding authors.

Declarations

Competing interests
The authors declare that they have no competing interests.

Author details
[1]BK21 FOUR R&E Center for Environmental Science and Ecological Engineering, Korea University, Anam-ro145, Seongbuk-Gu, Seoul 02842, Republic of Korea. [2]Department of Biology Science, Chosun University, 309 Pilmun-Daero, Dong-Gu, Gwangju 61452, Republic of Korea. [3]Division of Environmental Science and Ecological Engineering, Korea University, Anam-ro145, Seongbuk-Gu, Seoul 02842, Republic of Korea.

Received: 18 September 2022 Accepted: 10 November 2022
Published online: 27 November 2022

References
1. Aydin H, Azimi FC, Cook JD, Lee JE (2012) A convenient and general expression platform for the production of secreted proteins from human cells. J Vis Exp. https://doi.org/10.3791/4041
2. Pham PL, Kamen A, Durocher Y (2006) Large-scale transfection of mammalian cells for the fast production of recombinant protein. Mol Biotechnol 34(2):225–237. https://doi.org/10.1385/MB:34:2:225
3. Hunter M, Yuan P, Vavilala D, Fox M (2019) Optimization of protein expression in mammalian cells. Curr Protoc Protein Sci 95(1):e77. https://doi.org/10.1002/cpps.77
4. Kallunki T, Barisic M, Jaattela M, Liu B (2019) How to choose the right inducible gene expression system for mammalian studies? Cells. https://doi.org/10.3390/cells8080796
5. Gorochowski TE, Ignatova Z, Bovenberg RA, Roubos JA (2015) Trade-offs between tRNA abundance and mRNA secondary structure support smoothing of translation elongation rate. Nucleic Acids Res 43(6):3022–3032. https://doi.org/10.1093/nar/gkv199
6. Inouye S, Sahara-Miura Y, Sato J, Suzuki T (2015) Codon optimization of genes for efficient protein expression in mammalian cells by selection of only preferred human codons. Protein Expr Purif 109:47–54. https://doi.org/10.1016/j.pep.2015.02.002
7. Damaj MB, Jifon JL, Woodard SL, Vargas-Bautista C, Barros GOF, Molina J et al (2020) Unprecedented enhancement of recombinant protein production in sugarcane culms using a combinatorial promoter stacking system. Sci Rep 10(1):13713. https://doi.org/10.1038/s41598-020-70530-z
8. Fu H, Liang Y, Zhong X, Pan Z, Huang L, Zhang H et al (2020) Codon optimization with deep learning to enhance protein expression. Sci Rep 10(1):17617. https://doi.org/10.1038/s41598-020-74091-z
9. Zhou Z, Schnake P, Xiao L, Lal AA (2004) Enhanced expression of a recombinant malaria candidate vaccine in *Escherichia coli* by codon optimization. Protein Expr Purif 34(1):87–94. https://doi.org/10.1016/j.pep.2003.11.006
10. Phizicky EM, Hopper AK (2010) tRNA biology charges to the front. Genes Dev 24(17):1832–1860. https://doi.org/10.1101/gad.1956510
11. Dong J, Munoz A, Kolitz SE, Saini AK, Chiu WL, Rahman H et al (2014) Conserved residues in yeast initiator tRNA calibrate initiation accuracy by regulating preinitiation complex stability at the start codon. Genes Dev 28(5):502–520. https://doi.org/10.1101/gad.236547.113
12. Kozak M (1983) Comparison of initiation of protein synthesis in procaryotes, eucaryotes, and organelles. Microbiol Rev 47(1):1–45
13. RajBhandary UL (1994) Initiator transfer RNAs. J Bacteriol 176(3):547–552
14. Smith AE, Marcker KA (1970) Cytoplasmic methionine transfer RNAs from eukaryotes. Nature 226(5246):607–610
15. Drabkin HJ, RajBhandary UL (1985) Site-specific mutagenesis on a human initiator methionine tRNA gene within a sequence conserved in all eukaryotic initiator tRNAs and studies of its effects on in vitro transcription. J Biol Chem 260(9):5580–5587
16. Seong BL, RajBhandary UL (1987) *Escherichia coli* formylmethionine tRNA: mutations in GGGCCC sequence conserved in anticodon stem of initiator tRNAs affect initiation of protein synthesis and conformation of anticodon loop. Proc Natl Acad Sci USA 84(2):334–338
17. Ngo JT, Schuman EM, Tirrell DA (2013) Mutant methionyl-tRNA synthetase from bacteria enables site-selective N-terminal labeling of proteins expressed in mammalian cells. Proc Natl Acad Sci USA 110(13):4992–4997. https://doi.org/10.1073/pnas.1216375110
18. Tanrikulu IC, Schmitt E, Mechulam Y, Goddard WA 3rd, Tirrell DA (2009) Discovery of *Escherichia coli* methionyl-tRNA synthetase mutants for efficient labeling of proteins with azidonorleucine in vivo. Proc Natl Acad Sci USA 106(36):15285–15290. https://doi.org/10.1073/pnas.0905735106
19. Ngo JT, Champion JA, Mahdavi A, Tanrikulu IC, Beatty KE, Connor RE et al (2009) Cell-selective metabolic labeling of proteins. Nat Chem Biol 5(10):715–717. https://doi.org/10.1038/nchembio.200
20. Mahdavi A, Hamblin GD, Jindal GA, Bagert JD, Dong C, Sweredoski MJ et al (2016) Engineered aminoacyl-tRNA synthetase for cell-selective analysis of mammalian protein synthesis. J Am Chem Soc 138(13):4278–4281. https://doi.org/10.1021/jacs.5b08980
21. Bjork GR (1995) Genetic dissection of synthesis and function of modified nucleosides in bacterial transfer RNA. Prog Nucleic Acid Res Mol Biol 50:263–338
22. Tsai F, Curran JF (1998) tRNA(2Gln) mutants that translate the CGA arginine codon as glutamine in *Escherichia coli*. RNA (New York, NY) 4(12):1514–1522
23. Ling J, O'Donoghue P, Soll D (2015) Genetic code flexibility in microorganisms: novel mechanisms and impact on physiology. Nat Rev Microbiol 13(11):707–721. https://doi.org/10.1038/nrmicro3568
24. Lant JT, Berg MD, Sze DHW, Hoffman KS, Akinpelu IC, Turk MA et al (2018) Visualizing tRNA-dependent mistranslation in human cells. RNA Biol 15(4–5):567–575. https://doi.org/10.1080/15476286.2017.1379645
25. Govindan A, Ayyub SA, Varshney U (2018) Sustenance of *Escherichia coli* on a single tRNAMet. Nucleic Acids Res 46(21):11566–11574. https://doi.org/10.1093/nar/gky859
26. Yadavalli SS, Ibba M (2012) Quality control in aminoacyl-tRNA synthesis its role in translational fidelity. Adv Protein Chem Struct Biol 86:1–43. https://doi.org/10.1016/B978-0-12-386497-0.00001-3
27. Lagerkvist U, Rymo L, Waldenstrom J (1966) Structure and function of transfer ribonucleic acid. II. Enzyme-substrate complexes with valyl ribonucleic acid synthetase from yeast. J Biol Chem 241(22):5391–5400
28. Novelli GD (1967) Amino acid activation for protein synthesis. Annu Rev Biochem 36:449–484. https://doi.org/10.1146/annurev.bi.36.070167.002313
29. Brown MV, Reader JS, Tzima E (2010) Mammalian aminoacyl-tRNA synthetases: cell signaling functions of the protein translation machinery. Vascul Pharmacol 52(1–2):21–26. https://doi.org/10.1016/j.vph.2009.11.009
30. Pang YL, Poruri K, Martinis SA (2014) tRNA synthetase: tRNA aminoacylation and beyond. Wiley Interdiscip Rev RNA 5(4):461–480. https://doi.org/10.1002/wrna.1224
31. RajBhandary UL (2000) More surprises in translation: initiation without the initiator tRNA. Proc Natl Acad Sci USA 97(4):1325–1327. https://doi.org/10.1073/pnas.040579197
32. Eivazzadeh-Keihan R, Radinekiyan F, Maleki A, Salimi Bani M, Azizi M. new generation of star polymer: magnetic aromatic polyamides with unique microscopic flower morphology and in vitro hyperthermia of cancer therapy. 2020-01;v. 55.
33. Taheri-Ledari R, Zhang W, Radmanesh M, Mirmohammadi SS, Maleki A, Cathcart N et al (2020) Multi-stimuli nanocomposite therapeutic: docetaxel targeted delivery and synergies in treatment of human breast cancer tumor. Small 16(41):e2002733. https://doi.org/10.1002/smll.202002733
34. Maleki A, Hassanzadeh-Afruzi F, Varzi Z, Esmaeili MS (2020) Magnetic dextrin nanobiomaterial: an organic-inorganic hybrid catalyst for the synthesis of biologically active polyhydroquinoline derivatives by asymmetric Hantzsch reaction. Mater Sci Eng C Mater Biol Appl 109:110502. https://doi.org/10.1016/j.msec.2019.110502
35. Reuten R, Nikodemus D, Oliveira MB, Patel TR, Brachvogel B, Breloy I et al (2016) Maltose-binding protein (MBP), a secretion-enhancing tag for mammalian protein expression systems. PLoS ONE 11(3):e0152386. https://doi.org/10.1371/journal.pone.0152386

36. Park BJ, Kang JW, Lee SW, Choi SJ, Shin YK, Ahn YH et al (2005) The haploinsufficient tumor suppressor p18 upregulates p53 *via* interactions with ATM/ATR. Cell 120(2):209–221. https://doi.org/10.1016/j.cell.2004.11.054
37. Jun SY, Kang SH, Lee KH (2008) Fluorescent labeling of cell-free synthesized proteins with fluorophore-conjugated methionylated tRNA derived from in vitro transcribed tRNA. J Microbiol Methods 73(3):247–251. https://doi.org/10.1016/j.mimet.2008.02.016
38. Kang T, Kwon NH, Lee JY, Park MC, Kang E, Kim HH et al (2012) AIMP3/p18 controls translational initiation by mediating the delivery of charged initiator tRNA to initiation complex. J Mol Biol 423(4):475–481. https://doi.org/10.1016/j.jmb.2012.07.020
39. Kwon NH, Kang T, Lee JY, Kim HH, Kim HR, Hong J et al (2011) Dual role of methionyl-tRNA synthetase in the regulation of translation and tumor suppressor activity of aminoacyl-tRNA synthetase-interacting multifunctional protein-3. Proc Natl Acad Sci USA 108(49):19635–19640. https://doi.org/10.1073/pnas.1103922108
40. Kim JM, Seong BL (2017) Highly chromophoric Cy5-methionine for N-terminal fluorescent tagging of proteins in eukaryotic translation systems. Sci Rep 7(1):11642. https://doi.org/10.1038/s41598-017-12028-9
41. Petersson EJ, Shahgholi M, Lester HA, Dougherty DA (2002) MALDI-TOF mass spectrometry methods for evaluation of in vitro aminoacyl tRNA production. RNA (New York, NY) 8(4):542–547
42. Kim D, Cheon J, Yoon H, Jun HS (2021) Cudrania tricuspidata root extract prevents methylglyoxal-induced inflammation and oxidative stress *via* regulation of the pkc-nox4 pathway in human kidney cells. Oxid Med Cell Longev 2021:5511881. https://doi.org/10.1155/2021/5511881
43. Ibba M, Soll D (2000) Aminoacyl-tRNA synthesis. Annu Rev Biochem 69:617–650. https://doi.org/10.1146/annurev.biochem.69.1.617
44. Simsek M, Ziegenmeyer J, Heckman J, Rajbhandary UL (1973) Absence of the sequence G-T-psi-C-G(A)- in several eukaryotic cytoplasmic initiator transfer RNAs. Proc Natl Acad Sci USA 70(4):1041–1045
45. Chakraburtty K (1975) Primary structure of tRNA Arg II of *E. coli* B. Nucleic Acids Res 2(10):1787–1792
46. Delk AS, Rabinowitz JC (1974) Partial nucleotide sequence of a prokaryote initiator tRNA that functions in its non-formylated form. Nature 252(5479):106–109. https://doi.org/10.1038/252106a0
47. Walker RT, RajBhandary UL (1975) Formylatable methionine transfer RNA from Mycoplasma: purification and comparison of partial nucleotide sequences with those of other prokaryotic initiator tRNAs. Nucleic Acids Res 2(1):61–78
48. Miura M, Muranaka N, Abe R, Hohsaka T (2010) Incorporation of fluorescent-labeled non-alpha-amino carboxylic acids into the N-terminus of proteins in response to amber initiation codon. B Chem Soc Jpn 83(5):546–553. https://doi.org/10.1246/bcsj.20090320
49. Taira H, Hohsaka T, Sisido M (2006) In vitro selection of tRNAs for efficient four-base decoding to incorporate non-natural amino acids into proteins in an *Escherichia coli* cell-free translation system. Nucleic Acids Res 34(5):1653–1662. https://doi.org/10.1093/nar/gkl087
50. O'Donoghue P, Ling J, Wang YS, Soll D (2013) Upgrading protein synthesis for synthetic biology. Nat Chem Biol 9(10):594–598. https://doi.org/10.1038/nchembio.1339
51. Mahdavi A, Segall-Shapiro TH, Kou S, Jindal GA, Hoff KG, Liu S et al (2013) A genetically encoded and gate for cell-targeted metabolic labeling of proteins. J Am Chem Soc 135(8):2979–2982. https://doi.org/10.1021/ja400448f
52. Howard MT, Gesteland RF, Atkins JF (2004) Efficient stimulation of site-specific ribosome frameshifting by antisense oligonucleotides. RNA (New York, NY) 10(10):1653–1661. https://doi.org/10.1261/rna.7810204
53. Marquez V, Wilson DN, Tate WP, Triana-Alonso F, Nierhaus KH (2004) Maintaining the ribosomal reading frame: the influence of the E site during translational regulation of release factor 2. Cell 118(1):45–55. https://doi.org/10.1016/j.cell.2004.06.012
54. Hoffman RM, Erbe RW (1976) High in vivo rates of methionine biosynthesis in transformed human and malignant rat cells auxotrophic for methionine. Proc Natl Acad Sci USA 73(5):1523–1527. https://doi.org/10.1073/pnas.73.5.1523
55. Halpern BC, Clark BR, Hardy DN, Halpern RM, Smith RA (1974) The effect of replacement of methionine by homocystine on survival of malignant and normal adult mammalian cells in culture. Proc Natl Acad Sci USA 71(4):1133–1136. https://doi.org/10.1073/pnas.71.4.1133
56. Kokkinakis DM, Liu X, Chada S, Ahmed MM, Shareef MM, Singha UK et al (2004) Modulation of gene expression in human central nervous system tumors under methionine deprivation-induced stress. Cancer Res 64(20):7513–7525. https://doi.org/10.1158/0008-5472.CAN-04-0592
57. Warburg O (1956) On the origin of cancer cells. Science 123(3191):309–314. https://doi.org/10.1126/science.123.3191.309
58. Rocha CM, Barros AS, Goodfellow BJ, Carreira IM, Gomes A, Sousa V et al (2015) NMR metabolomics of human lung tumours reveals distinct metabolic signatures for adenocarcinoma and squamous cell carcinoma. Carcinogenesis 36(1):68–75. https://doi.org/10.1093/carcin/bgu226
59. Urasaki Y, Heath L, Xu CW (2012) Coupling of glucose deprivation with impaired histone H2B monoubiquitination in tumors. PLoS ONE 7(5):e36775. https://doi.org/10.1371/journal.pone.0036775
60. Bjork GR, Jacobsson K, Nilsson K, Johansson MJ, Bystrom AS, Persson OP (2001) A primordial tRNA modification required for the evolution of life? EMBO J 20(1–2):231–239. https://doi.org/10.1093/emboj/20.1.231
61. Okamoto T, Kawade Y (1967) Electrophoretic separation of complexes of aminoacyl-tRNA synthetase and transfer RNA. Biochem Biophys Acta 145(3):613–620
62. Zhou Z, Sun B, Nie A, Yu D, Bian M (2020) Roles of aminoacyl-tRNA synthetases in cancer. Front Cell Dev Biol 8:599765. https://doi.org/10.3389/fcell.2020.599765
63. Yu YC, Han JM, Kim S (2021) Aminoacyl-tRNA synthetases and amino acid signaling. Biochim Biophys Acta Mol Cell Res 1868(1):118889. https://doi.org/10.1016/j.bbamcr.2020.118889
64. Koubek J, Chen YR, Cheng RP, Huang JJ (2015) Nonorthogonal tRNA(cys) (Amber) for protein and nascent chain labeling. RNA (New York, NY) 21(9):1672–82. https://doi.org/10.1261/rna.051805.115
65. Masuda I, Igarashi T, Sakaguchi R, Nitharwal RG, Takase R, Han KY, et al (2017) A genetically encoded fluorescent tRNA is active in live-cell protein synthesis. Nucleic Acids Res 45(7):4081–93. https://doi.org/10.1093/nar/gkw1229
66. Terasaka N, Hayashi G, Katoh T, Suga H (2014) An orthogonal ribosome-tRNA pair via engineering of the peptidyl transferase center. Nat Chem Biol 10(7):555–7. https://doi.org/10.1038/nchembio.1549
67. Quast RB, Mrusek D, Hoffmeister C, Sonnabend A, Kubick S (2015) Cotranslational incorporation of non-standardamino acids using cell-free protein synthesis. FEBS Lett 589(15):1703–12. https://doi.org/10.1016/j.febslet.2015.04.041
68. Thoring L, Wustenhagen DA, Borowiak M, Stech M, Sonnabend A, Kubick S (2016) Cell-Free Systems Based on CHO Cell Lysates: Optimization Strategies, Synthesis of "Difficult-to-Express" Proteins and Future Perspectives. PLoSOne 11(9):e0163670. https://doi.org/10.1371/journal.pone.0163670
69. Barhoom S, Kaur J, Cooperman BS, Smorodinsky NI, Smilansky Z, Ehrlich M, et al (2011) Quantitative single cell monitoring of protein synthesis at subcellular resolution using fluorescently labeled tRNA. Nucleic Acids Res 39(19):e129. https://doi.org/10.1093/nar/gkr601
70. Dittmar KA, Goodenbour JM, Pan T (2006) Tissue-specific differences in human transfer RNA expression. PLoS Genet 2(12):e221. https://doi.org/10.1371/journal.pgen.0020221

Publisher's Note